3/19/2012

Ultrasonic Phased Array Evaluation of Control Rod Drive Mechanism (CRDM) Nozzle interference fit and weld region – NDE Results and Destructive Analysis*

A. D. Cinson, S. L. Crawford, P. J. MacFarlan, B.D. Hanson, R. A. Mathews
Pacific Northwest National Laboratory, 902 Battelle Blvd., P.O. Box 999, Richland, WA 99352

ABSTRACT

In this investigation, non-destructive and destructive testing were used to evaluate potential boric acid leakage paths around an Alloy 600 CRDM penetration (Nozzle 63) from the North Anna Unit 2 reactor pressure vessel head that was removed from service in 2002. A previous volumetric examination of this nozzle sponsored by the Electric Power Research Institute identified a probable leakage path in the interference fit between the penetration and the vessel head but this was not confirmed by destructive analysis. Subsequently, Nozzle 63 was made available for independent tests which PNNL conducted. For this investigation, Nozzle 63 was examined using phased array ultrasonic testing (UT) with an immersion eight element annular 5.0 MHz probe from the nozzle inner diameter. Prior to examining Nozzle 63, a CRDM penetration mockup with known electrical discharge machining notches and boric acid deposits was used to assess probe sensitivity and resolution. Responses from the mock-up specimen were evaluated to determine detection limits and characterization capability as well as to contrast the ultrasonic response differences with and without the presence of boric acid in the interference fit region. Following the ultrasonic non-destructive testing of Nozzle 63, the nozzle was destructively examined to visually assess the leak paths. These destructive and nondestructive results are compared and results are presented.

Keywords: Nondestructive Testing, Ultrasonic, Phased Array, Control Rod Drive Mechanism, Leak Path Assessment

1. INTRODUCTION

Research is being conducted for the U.S. Nuclear Regulatory Commission (NRC) at the Pacific Northwest National Laboratory (PNNL) to assess the effectiveness and reliability of advanced nondestructive examination (NDE) methods. Primary water stress corrosion cracking (PWSCC) in nickel-base alloy primary pressure boundary components may be a safety concern due to the potential for reactor pressure boundary leaks, the associated potential of boric acid corrosion of low alloy steels, and the development of flaws in piping or welds. Alloy 690 and its associated weld metals, Alloy 52 and 152, have been used in replacement pressurized water reactor (PWR) components to reduce PWSCC susceptibility[1,3]

While more than 30 head replacements have occurred at operating PWRs, only a limited number of materials that have actually been in service are available for characterization and testing. In the 2001 refueling outage, some of the North Anna Unit-2 nozzles were repaired using Alloy 52/152 including Nozzles 63 and 51. In the 2002 refueling outage, 63 of 65 J-groove welds had flaw indications and cracking in 42 of these welds was severe enough to require repair. At that time, the utility decided to replace the reactor head. Previously, the Electric Power Research Institute (EPRI) sponsored the removal and analysis of several nozzles. Currently, Nozzles 63, 51, and 10 are in storage at PNNL. Some prior characterizations of Nozzle 63 were performed and revealed a probable leak path and indications on the outside diameter of the nozzle tube. Surface examinations of the J-groove weld identified axial indications.

Previous testing on material removed from the Davis-Besse reactor head provided valuable information regarding crack growth rates of CRDM nozzle materials and welds. The Alloy 600 CRDM nozzles from Davis-Besse were determined to be highly susceptible to PWSCC whereas the Alloy 82/182 J-groove weld metal had lower than average susceptibility based on measured PWSCC growth rates [1,5]. Unlike the Davis-Besse CRDM nozzles, many of the cracks identified in the North Anna Unit-2 nozzle penetrations were located in the Alloy 82/182 J-groove weld and butter material. Some of the North Anna-2 CRDM nozzles including Nozzle 63 were repaired using an Alloy 52 weld overlay.

Deleted: cability

Deleted: significant

Deleted: These conditions, depending on the size and location of the flaws, could result in a significant loss-of-coolant accident.

B/36

A previous leak path assessment was conducted on Nozzle 63. It is of interest to conduct additional nondestructive assessments to characterize the leak path followed by destructive analysis and a comparison to the nondestructive examination.

2. MOCKUP SPECIMEN

2.1 Design

The CRDM mock-up calibration specimen consists of several components; mainly, the Inconel tube with flange, and two 6-in. carbon steel blocks. The design of this calibration specimen is to mimic the interference fit conditions between the Inconel tubing and the reactor vessel head (RVH) material as found in a PWR. The mock-up assembly employs similar materials and practices as utilized in the assembly of an actual RVH; however, this mock-up has two interference fit regions (Figure 1). One region, top block, contains EDM notches to establish an ultrasonic resolution and calibrated response from known voids. The second region, bottom block on this specimen, has boric acid deposits strategically placed in the fit to simulate a leakage path with boric acid deposits. Figure 1 graphically illustrates the assembled orientation of the specimen.

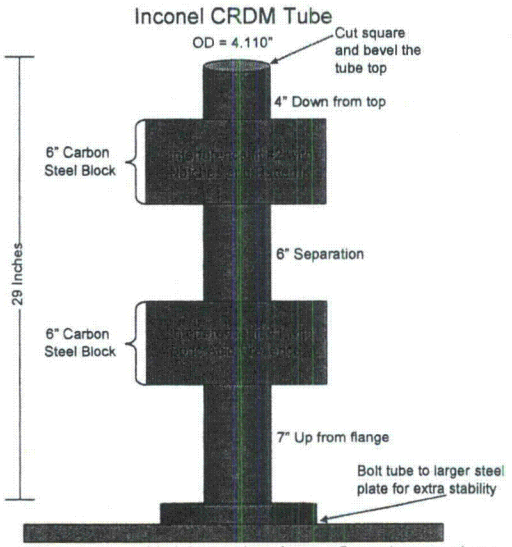

Figure 1. Assembled CRDM interference fit mock-up specimen

Boric Acid Presence: Interference fit #1 contains boric acid deposits in the region where the Inconel tube meets the carbon steel block. The boric acid deposits are associated with a leaking nozzle assembly in the field. The water inside an RVH contains a certain amount of boric acid that acts as a neutron absorber for controlling the nuclear reaction. Under pressure, some of this contaminated water can leak past the CRDM seal weld at the wetted surface and into the interference fit region. With the extreme heat from the reactor, the water evaporates leaving behind the solid boric acid. During in-service evaluations of CRMD interference fits, the presence of boric acid has been shown to create a unique ultrasonic transmission and reflection pattern based upon the acid presence [1,4]. The mock-up is an attempt to simulate that very phenomenon.

The objective of this fit region was to create conditions where there are both regions of boric acid and where there was a lack of acid. Ideally, the contrast of the two regions in the ultrasonic data will reveal differences in ultrasonic transmission/reflection. The process of creating the simulated leakage paths with boric acid began with masking off regions on the Inconel tube outer diameter (OD) where boric acid was unwanted with masking tape. The boric acid was prepared for application by mixing a small amount of boric acid in solid form with a small amount of methanol. The two

components were mixed into a paste with medium to high viscosity. The application of the acid involved spreading a thin and even coat of the paste with a compatible brush over the localized region on the OD of the tube between the masked off sections in a pattern as observed in Figure 2. Upon solidification of the boric acid, the masking tape was removed. Further, a snake-like pattern was scraped into a boric acid region as indicated with the blue line in Figure 2.

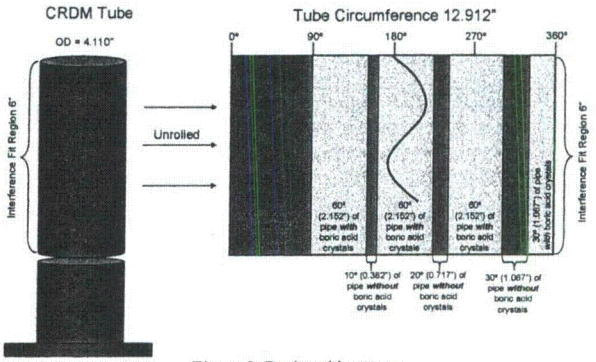

Figure 2. Boric acid pattern

EDM Notches and Patterns: The second interference fit contains various precision-crafted EDM notches (Figure 3) in the fit region. These notches were ultrasonically characterized to determine detection limits and image resolution.

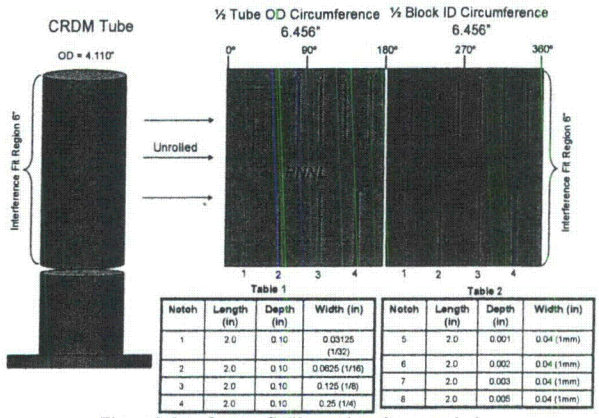

Table 1

Notch	Length (in)	Depth (in)	Width (in)
1	2.0	0.10	0.03125 (1/32)
2	2.0	0.10	0.0625 (1/16)
3	2.0	0.10	0.125 (1/8)
4	2.0	0.10	0.25 (1/4)

Table 2

Notch	Length (in)	Depth (in)	Width (in)
5	2.0	0.001	0.04 (1mm)
6	2.0	0.002	0.04 (1mm)
7	2.0	0.003	0.04 (1mm)
8	2.0	0.005	0.04 (1mm)

Figure 3. Interference fit #2; notch and pattern design

This interference fit focuses on notches/patterns placed on the Inconel tube OD (silver colored region in Figure 3) as well as notches placed in the carbon steel block (represented by the brown/orange color in the figure). The first 180 degrees of the assembly had the notches cut into the tube OD and from 180 to 360 degrees had the notches cut into the carbon steel block ID. A theoretically determined spot size using the 5-MHz phased-array (PA) probe at the interference fit region is 1.8 mm (0.071 in.) in both x and y directions (circumferential and axial directions). For reference, the theoretical wavelength (λ) in the Inconel tube material at 5 MHz is 1.1 mm (0.043 in.). The probe resolution in both the circumferential and axial directions was measured by acquiring data on a series of notches 2 mm wide × 2 mm deep × 25 mm long (0.079 in. × 0.079 in. × 1.0 in.) that are spaced 2, 3, and 5 mm (0.079, 0.12, and 0.20 in.) apart (approximately 2, 3, and 5 λ). One set of these notches was orientated circumferentially and the other was oriented axially represented by blue lines in Figure 3. To measure detection sensitivity, axial notches 1–4 were placed equidistant from each other and had a constant depth while the widths varied from 0.7938 to 6.35 mm (0.03125 to 0.25 in.) wide, simulating potential

leakage paths. The third set of notches was for depth sensitivity determination andwas also placed axially and equidistant from each other. These are notches 5–8 and have consistent lengths and widths but varied in depth. These three sets of notches did not overlap, so ultrasonic observations were made independently for resolution (the ability to resolve two closely spaced indications) and width and depth sensitivity. The acronym 'PNNL' was also notched on the OD of the tube for uniqueness and provided an indication of off-axis sensitivity.

2.2 Mockup Specimen (Assembly)

The assembly of this mock-up specimen involved temporarily shrinking the Inconel tube to accept the carbon steel blocks that were precisely machined with a hole that was 3 mils smaller than the OD of the Inconel tube when all components were at a room temperature of 22°C (72°F). This created an interference fit of 3 mils after all components returned to room temperature [2].

The expected amount of thermal reduction was calculated for the nozzle and then later experimentally measured. Thermal expansion coefficients are generally given in tabular form for different materials over a given temperature range. These table values assume a linear relationship over a limited temperature range. Cryogenic material properties were needed for the temperatures used in forming the interference fit. Two reference papers discussed material properties of metal alloys at cryogenic temperatures. Inconel 718 was one of the material studied and represented the nozzle material for our calculated material shrinkage estimates. To form the interference fit, the nozzle was taken from room temperature, 293°K, to the temperature of liquid nitrogen, 77.2° K. Clark [6] measured the thermal expansion coefficients from liquid hydrogen temperature to room temperature, 20°K to 293°K, in 10 or 20 degree steps for different metallic alloys. Results are presented in tabular form for the expansion relative to room temperature. From the table for Inconel 718 at 80°K:

$$223 = [(L293 - L80) / L293] \times 105 \quad (1)$$

expansion relative to room temperature

The calculated expansion from Eq. (1) gives a shrinkage value of 0.232 mm (0.00914 in.) for a 104.14 mm (4.1in.) -long section of Inconel 718 material.

Marquardt [7] models the material properties over a large temperature range (4 to 300°K) with a polynomial or a logarithmic polynomial equation. An equation for the integrated linear thermal expansion or change in length is given as:

$$(LT - L293) / L293 = (a + bT + cT2 + dT3 + eT4) \times 10^{-5} \quad (2)$$

The coefficients for 718 Inconel are listed as:

a = −2.366E+02 d = −7.164E-06
b = −2.218E-01 e = 0
c = 5.601E-03

From this equation the expansion relative to room temperature for a temperature of 77°K was calculated to be 223.74×10^{-5}. Applying this value to a 104.14 mm (4.1 in.) length of Inconel produces a shrinkage value of 0.233 mm (0.00917 in.) This result very closely matches the result from Eq. (1) given above.

3. ULTRASONIC PHASED ARRAY INSPECTION

3.1 Phased Array Probe

The specimens were examined with a pulse-echo (PE) longitudinal phased-array probe with a center frequency of 5 MHz. The PA probe was designed in a 1-D annular configuration using eight elements. The probe contains elements in a Fresnel radius pattern starting with a radius of 3 mm (0.12 in) up to the final element radius of 9.72 mm (0.38 in). Thus, the total aperture is 296.81 mm^2 (0.46 in^2). The probe exhibits a 72% bandwidth at −6 decibels (dB). This particular design was chosen for enhanced depth focusing capabilities. Its beam forming capabilities have been modeled to show a satisfactory notification of the interference fit region of interest as well as the ability to propagate a uniform ultrasonic beam deep into the weld region.

3.2 Focal Law Development

Before a PA probe can be used to perform an examination, a set of focal laws must be produced to control the firing of individual elements which in turn form a beam. The focal laws are inputs to the Ultravision control software, which determines specific elements to excite at specific times to allow for proper beam-forming in the material to be examined. The focal laws also contain details about the angles being generated, the focal point of the sound field, the delays associated with the wedge and electronics, and the orientation of the probe. PNNL uses a software package contained in the Ultravision 1.2R4 software program for producing focal laws known as the "ZETEC Advanced Focal Law Calculator." The software package performs two functions: (1) focal law generation and (2) simulation of the ultrasonic field produced by the probe when using the generated laws. The user enters the physical information about the PA probe, such as the number of elements, the sizes of the elements, and the wedge information, such as the wedge angle and the wedge size, into the program. The desired angles and focal distances are then entered, and the software generates the needed delays for each element to produce the desired beam steering and focusing in the material. The software beam simulation produces a simple image of the probe on the wedge, ray-tracing to show the focal depth and steering desired, and density mapping to enable the viewer to see how well the sound field responds for a particular angle and whether grating lobes exist that may be detrimental to the examination. Figure **Error! Reference source not found.** shows an example of the ray tracing for a probe on the left with the sound field density mapping on the right for a particular depth. It should be noted that this simulation is performed in isotropic material; that is, the velocity of sound is maintained throughout any angle for a particular wave mode.

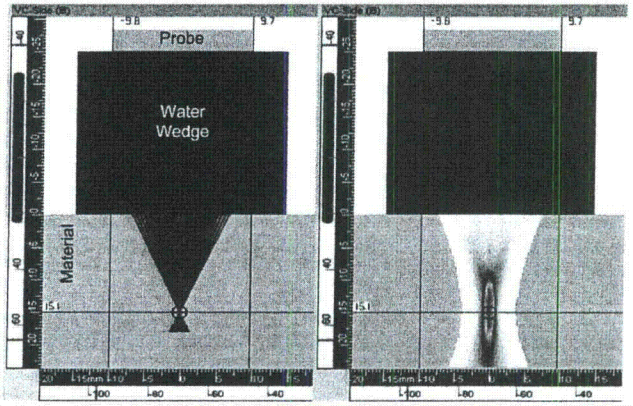

Figure 4: Side View—Left: Law Formation. Right: Sound Field Simulation for a Depth Focus of 15 mm (0.59 in.). Blue and red lines are measurement cursors from the origin defined as center of probe in X,Y and material face in Z.

3.3 Ultrasonic Phased Array Configuration

Set-up and laboratory configuration for PA-ultrasonic testing (UT) data acquisition on the mockup specimen and. Nozzle 63 required the use of a custom slave-encoded scanner to be mounted on the specimen. The scanner has two stepper motors that control the axes of movement; circumferentially around the specimen and vertical in the axial direction of the specimen. Attached to the motor shafts are slave encoders that provide circumferential and axial position information to the PA electronics. The scanner was attached to the tube by sliding the scanner over the tube and the three set screws were tightened. This provided easy manipulation for fine-tuning of the alignment of the scanner for optimum phased-array data collection. The setup is shown in Figure 4 with the scanner on the calibration specimen. The probe was mounted on an extension arm that is adjustable along the pipe axis for easy adjustment to scan the region of interest.

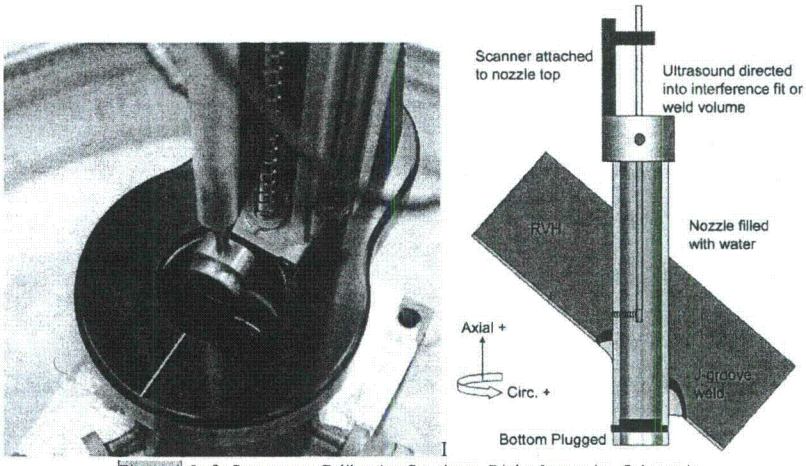

Figure 4. Left: Scanner on Calibration Specimen. Right: Inspection Schematic

Comment [PGO1]: The previous figure was labeled Figure 4. Think this should be figure 5. Check all the figure captions and text references to make sure they're correct.

Water filled the tube to establish adequate acoustic coupling between the probe and the specimen ID surface. Data acquisition was accomplished using the ZETEC Tomoscan III system. This commercially available system is equipped to accommodate a maximum of 64 channels from PA probes and requires the use of Ultravision 1.2R4 software. Its frequency pulsing electronics will drive probes in the 0.5–20 MHz range. Phased-array data were acquired over a range of inspection depths from 1–15 mm (0.039 – 0.59 in.) at a normal or 0° angle of inspection. Raster data were acquired at 0.25 degree in the scan and 0.5-mm (0.019 in.) increment in the index on the calibration specimen and 0.5 degree in the scan and 0.5-mm (0.019 in.) increment in the index for Nozzle 63. The scan axis was defined as the circumferential direction around the tube and the index defined as the axial travel up or down the tube.

4. PHASED ARAY DATA AND ANALYSIS (CALIBRATION SPECIMEN)

4.1 Notch Regions

Data were acquired on the calibration mockup assembly with the ultrasonic PA probe. The notch pattern was machined into the ID of the carbon steel material in the 180 to 360 degree range and in the Inconel tube OD over the 0 to 180 degree range. The axial resolution notches are in the upper left region. Just below are the circumferential resolution notches. The upper right contains notches that vary in depth and the lower notches vary in width.

The Inconel tube notched area was scanned over approximately a 0 to 170 degree range in the circumferential direction and 10 to 180 mm (0.39 to 7.09 in.) in the axial direction with the data image shown in Figure 6. This top view or C-scan image displays the resolution notches in the upper left portion of the image. The variable depth and width notches are also seen as well as the "PNNL" letters.

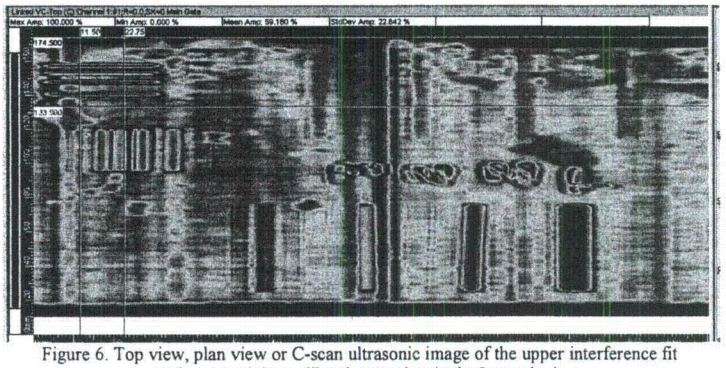

Figure 6. Top view, plan view or C-scan ultrasonic image of the upper interference fit region containing calibration notches in the Inconel tube

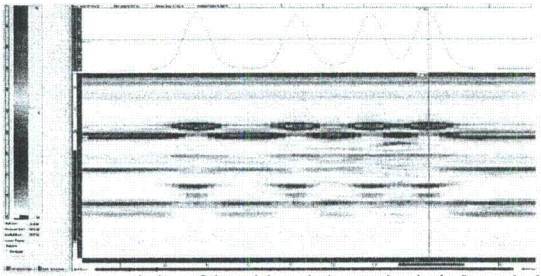

Figure 7. D-scan end view of the axial resolution notches in the Inconel tube

The axial resolution notches were gated or selected for analysis. An enlarged end view depicted in Figure 7 was used to measure the center-to-center spacing of the notches. From this view an "echo dynamic" line or profile was drawn through the upper part of the notches' responses and plotted at the top of the image. The notch widths left to right as measured at the half amplitude points are 2, 2, 2.5, and 2.5 mm (0.08, 0.08, 0.10, and 0.10 in.). The true widths are 2.03 mm (0.80 in.) for all four notches. Notch depths were measured at 2 mm, which agrees with the true depth of 2.03 mm (0.08 in.) for all four notches. Finally, the notches were separated from each other providing an indication of probe resolution in the axial direction. In this set of notches, the center-to-center true-state separation is 7.11, 5.08, and 4.06 mm (0.28, 0.20, and 0.16 in.). The corresponding measurements are 7.0, 5.5, and 4.0 mm (0.28, 0.22, and 0.16 in.) indicating a better than 4.0 mm (0.16 in.) axial resolution. The circumferential resolution notch set was also analyzed and showed a probe circumferential resolution of approximately 4.4 mm (0.17 in.).

The set of notches in the upper right portion of the scanned image (Figure 6) vary in depth, from 0.028 to 0.124 mm (0.0011 to 0.0049 in.). The center-to-center spacing of the flaws measures 23.84, 24.29, and 23.61 mm (0.94, 0.96, 0.93 in.) whereas the true spacing is 25.4 mm (1.0 in.). Flaw depths were not measurable but these shallow flaws were detected. Higher frequency may be needed to resolve the depths of these notches.

The final set of notches contained width variations and are shown in Figures 8 and 9.These flaws were measured with depths of 2.2, 2.5, 2.7, and 2.9 mm (0.09, 0.10, 0.11, and 0.11 in.), left to right in the image, while true state is 2.53 mm (0.10 in.) for all notches. The widths of the flaws were measured in two ways. The first used the width of the upper part of the flaw response and the second used the width of the loss of back-wall signal. The loss of back-wall signal was more accurate with empirical width values of 2.52, 3.21, 3.90, and 7.56 mm. True state is 0.79, 1.59, 3.18 and 6.35 mm (0.03, 0.06, 0.13, and 0.25 in.). When measured from the second ultrasonic back-wall echo, the loss of signal measurements give notch widths of 0.917, 2.521, 3.896, and 6.417 mm (0.036, 0.099, 0.153, and 0.253 in.), which are better representations of true state.